Canadian Conference - Pacific Conference on Earthquake Engineering 2023
Vancouver, British Columbia
June 25th – June 30th, 2023

Shape Memory Alloys in Reinforced Concrete Walls: Ongoing Work and Future Directions

Ryan Hoult[1*], Olga Klinkova[2], Matthieu Lezaack[1], Stefania Lo Feudo[2], Aude Simar[1], and João Pacheco de Almeida[1]

[1]Institute of Mechanics, Materials and Civil Engineering, UCLouvain, Louvain-la-Neuve, Belgium
[2]QUARTZ Laboratory (EA7393), ISAE-Supméca, Saint-Ouen-sur-Seine, France
*ryan.hoult@uclouvain.be (Corresponding Author)

ABSTRACT

An increasing number of structures, namely bridges and buildings, rely on reinforced concrete (RC) walls as seismic-resisting systems. Therefore, their design is pushed to accompany the major societal concerns, building owner requests, and scientific advances. In particular, longer service lives – with consideration of durability issues, together with more refined seismic performance criteria – which go well beyond collapse prevention or life safety, need to be considered. The minimisation of residual displacements has become an important performance criterion for the post-earthquake repairability and serviceability of structures. Substituting locally reinforcing steel rebars with Shape Memory Alloy (SMA) reinforcement within a plastic hinge region has been offered as a potential solution to address this issue. This paper starts by presenting some recent, as well as planned, experimental and numerical research investigations for the implementation of SMAs bars in steel-reinforced RC walls. They include: (i) a novel connection method between steel and SMA bars, using inertia friction welding, which provides promising results to avoid the use of mechanical couplers, (ii) recent advanced numerical modelling of walls with SMA rebars with a focus on the simulation of residual displacements, (iii) some comments on the foreseen application of cost-effective iron-based superelastic SMA rebars, which will be explored in an upcoming project, and (iv) an overview of an upcoming (end of 2023) shake-table test of a 40-ton large-scale RC U-shaped core wall detailed with SMA rebars. To address durability and longer service lives of structures, the employment of fibre-reinforced polymer (FRP) rebars in RC construction has been steadily growing. This paper concludes by mentioning some of the authors' work on this front, including: (i) the development of a novel hybrid composite FRP-SMA – alleviating some of the material disadvantages of the existing FRP rebar materials, and (ii) an upcoming test program of walls detailed with GFRP and SMA reinforcement.

Keywords: SMA, walls, recentering, performance-based, GFRP, residual displacements

INTRODUCTION

Presently, concrete is the most used building material in the world [1], and the second most-consumed material in the world after water [2]. When combined with steel bars, reinforced concrete (RC) is strong in both tension and compression and can exhibit ductility in rare events, such as earthquakes. These are just some of the qualities that have made RC construction the most popular type of structure in the world [3]. There is an expectation that cement production and RC construction will continue at an ever-increasing rate, including: (i) population growth, which is estimated to increase by 2 billion between now and 2050 [4]; (ii) rapid urbanisation, where in 1950, just 30% of the world's population lived in urban settlements, whereas it is projected that, by 2050, 68% of the world's approximate 10 billion inhabitants will be urban dwellers [4]; and (iii) economic development, particularly in regions with projected economic growth, such as Southeast Asia. Thus, the number of buildings worldwide is expected to double by 2060 [5], and it is likely that the majority of these structures will be made of RC. While there are some appealing qualities in the use of RC for infrastructure, there are also some critical challenges that need to be urgently overcome to achieve sustainable and resilient future cities.

One of the major challenges is that RC structures are a significant source of carbon dioxide (CO_2) emissions. The annual production of the most widely applied binder and construction material, Portland cement and cement concrete, has reached 4.1 billion tons [6] and 25 billion tons, respectively [7]. To put that into context, the global carbon footprint of the cement industry is approximately 7-8% [8], and this number is expected to grow. Recent studies have suggested that buildings offer the greatest abatement opportunities for reducing greenhouse gas emissions [9]. Other challenges, among many, include an increase of the seismic risk of RC buildings internationally, primarily due to (i) a significant population growth in earthquake-prone urban regions, with many non- or unsuitably-engineered buildings in low and middle-income countries, and (ii) the rising vulnerability of ageing infrastructure [10], where corrosion can affect the resilience of the structural system to seismicity [11, 12]. Regarding the former, the global population boom of recent decades has resulted in the expansion of urban areas that have created densely populated cities in close proximity to large, active faults, significantly increasing the exposure of people and assets in general to the risk of seismic events [13]. In fact, from 2000 to 2015, there were more fatalities from earthquakes than from any other natural disaster, killing on average 45,000 people per year [14]. For the same period, the economic impact of earthquakes accounted for 1.85 thousand billion US dollars (US$ 1.85 x 10^{12}), which corresponds to approximately 27% of the total economic losses from all-natural disasters [14]. Some of these estimated costs can be directly attributed to excessive post-earthquake residual displacements in RC buildings, which can result in the demolition of the structure after being declared "uneconomic to repair". Large, post-earthquake residual displacements (i.e., the permanent relative deformation of a structure with respect to its foundation) impose very costly repairs and can require the demolition and reconstruction of the entire building. For example, approximately 25% of all buildings in the central business district (CBD) of Christchurch were no longer vertical after the 2010-2011 earthquake sequence in New Zealand [15]. Many of these building tilts were in such excess that they required demolition after being declared "uneconomic to repair", where 60% of RC buildings with 3+ stories were demolished [16]. Another example is the 1995 Kobe earthquake [17] in Japan, where almost 100 bridge columns were observed to have noticeable permanent deformation that required demolition and replacement, resulting in large economic losses [18]. In fact, significant damage to RC buildings and bridges, resulting in the demolition of many structures, has been observed in many other recent earthquake events, including (but not limited to) the 1985 Mexico City earthquake [19] in Mexico, the 1994 Northridge earthquake [20] in the United States, the 2009 L'Aquila earthquake [21] in Italy, the 2010 Maule earthquake [22] in Chile, or more recently during the destructive earthquakes of south-east Turkey in February 2023.

Regardless of the variety of solutions that will be used to overcome some of these challenges, new buildings will need to be designed for significantly longer service lives [23]. Extending the lifetime of buildings is estimated to account for about one-third of steel demand reduction in a sustainable development scenario for 2050 [24]. Such values increase if complemented by improved building design, emphasising that maximising the design life of buildings and infrastructure can also significantly lower the cement demand. However, constructing longer-lasting infrastructure presents a challenge regarding material durability. There is significant research and development currently underway to develop the next generation of concrete technology, which can reduce the carbon footprint of the structure and increase durability. Various substitutes to reinforcing steel are also being investigated, including corrosion resistant materials such as fibre reinforced polymers and superelastic shape memory alloys (SMAs). The need to extend the design lifetime of infrastructure also suggests an increase in the design seismic action. For example, if current design and construction practices continue (i.e., no increase in durability), the probability of a structure reaching (or exceeding) the collapse performance level with a service life extension, say, from 50 to 100 years, will approximately double. If the service life is extended to 150 years, it triples. Thus, in view of the continuous growth of population and overall life quality, it is pressing to reform the construction sector by increasing the seismic resilience of reinforced concrete structures and simultaneously reducing their maintenance, strengthening, and retrofit costs.

This paper presents some recent and planned (future) experimental and numerical research investigations conducted by the authors for the implementation of SMA rebars in steel-reinforced RC walls. This type of lateral load resisting system is among the most popular used in construction practices internationally for effectively resisting wind and earthquake actions of mid- and high-rise buildings. The overarching aim and objective of the following summarised research projects is essentially the same: to design, develop, and test novel, sustainable, and economically competitive substitute materials for reinforcing robust RC wall structures that can minimise residual displacements and increase the lifespan of the structure, leading to a much-needed (r)evolution in the seismic design of engineering structures.

CURRENT RESEARCH

Inertia Friction Welding

Shape memory alloys (SMAs), in particular nickel titanium (NiTi) SMAs, currently remain an expensive material [25]. As such, detailing SMA rebars throughout the entire height of a RC cantilever wall is both impractical and unnecessary. Performance-based design of RC walls typically involves the design of a single plastic hinge to form at the base of the wall, where the reinforcement in the outermost regions of the cross-section (i.e., the boundary regions) commonly controls the bending actions. Thus, SMA rebars in walls can be placed at the base, over a restricted length equivalent to the plastic hinge, and in the extreme tension fibre regions. This type of reinforcement design detailing would result in an extremely reduced required quantity of SMA rebars in wall buildings, particularly in comparison to the detailing required for frame structures [25], and therefore a negligible overall construction cost increase can be expected. One difficulty with this proposed design is an efficient and rigid connection between the SMA and steel rebars.

Mechanical couplers have typically been used in previous experimental studies to connect the shape memory alloys to the reinforcing steel. In fact, to the author's knowledge, all previous tests on RC walls detailed with SMA rebars [25-28] have used mechanical couplers to connect the SMA rebars to conventional steel reinforcement. It appears that the use of couplers has also been unavoidable for all beams, columns, and beam-column joints tested up to now [29]. There are, however, some challenges with the use of couplers in practice, including a reduction of RC member displacement capacity [30]; for example, up to 43% reduction has been reported when using mechanical couplers compared to unspliced members. Furthermore, the use of long, thick, and rigid couplers can restrict the rotation capacity of the RC member [31] and also impose some difficulties with regards to member detailing, including increased concrete covers and providing closely spaced confining reinforcement. Slippage inside the couplers has also been reported in several experimental tests [29]. It is for the above reasons that the current seismic codes prohibit the use of mechanical couplers within the plastic hinge regions of RC structures.

Thus, to avoid the use of couplers, the authors are currently developing a novel connection between SMA and steel rebars. A recent publication by some of the authors [32] demonstrates that a full-strength connection between NiTi SMA to conventional steel bars is possible through friction welding methods. While the performance of these connections has only been validated under quasi-static tensile monotonic loading [32], their response under dynamic, reverse-cyclic and fatigue loading is the subject of ongoing and future investigations, both under uniaxial tensile-compressive loading and as reinforcing rebars in RC structural members. The exploration of other materials within the SMA material family, namely iron-based, is also envisaged (discussed more in the Future Research section of this paper). The influence of the distinct axial stiffness between SMA and steel rebars on the evolution of the strain profiles along the length of RC walls – and its implications on structural performance and modelling – is also under investigation.

Numerical Simulations of RC SMA walls

A recent investigation by some of the authors examined the residual displacement of RC walls, detailed with either steel or SMA reinforcement, using a large database of walls and conducted a parametric study using finite element (FE) modelling analyses [33]. For this task, VecTor2 [34] was employed, a state-of-the-art nonlinear FE modelling program for plane RC sections that is based on the disturbed stress field model (DSFM) [35]. In the accompanying paper [33], the authors validate the material models employed using the results from three separate experimental campaigns. The numerical results for just one of these experimental campaigns are summarised here, where the interested reader can read more results and information on the methodology of the research investigation, material models employed, and other modelling assumptions in the corresponding publication [33].

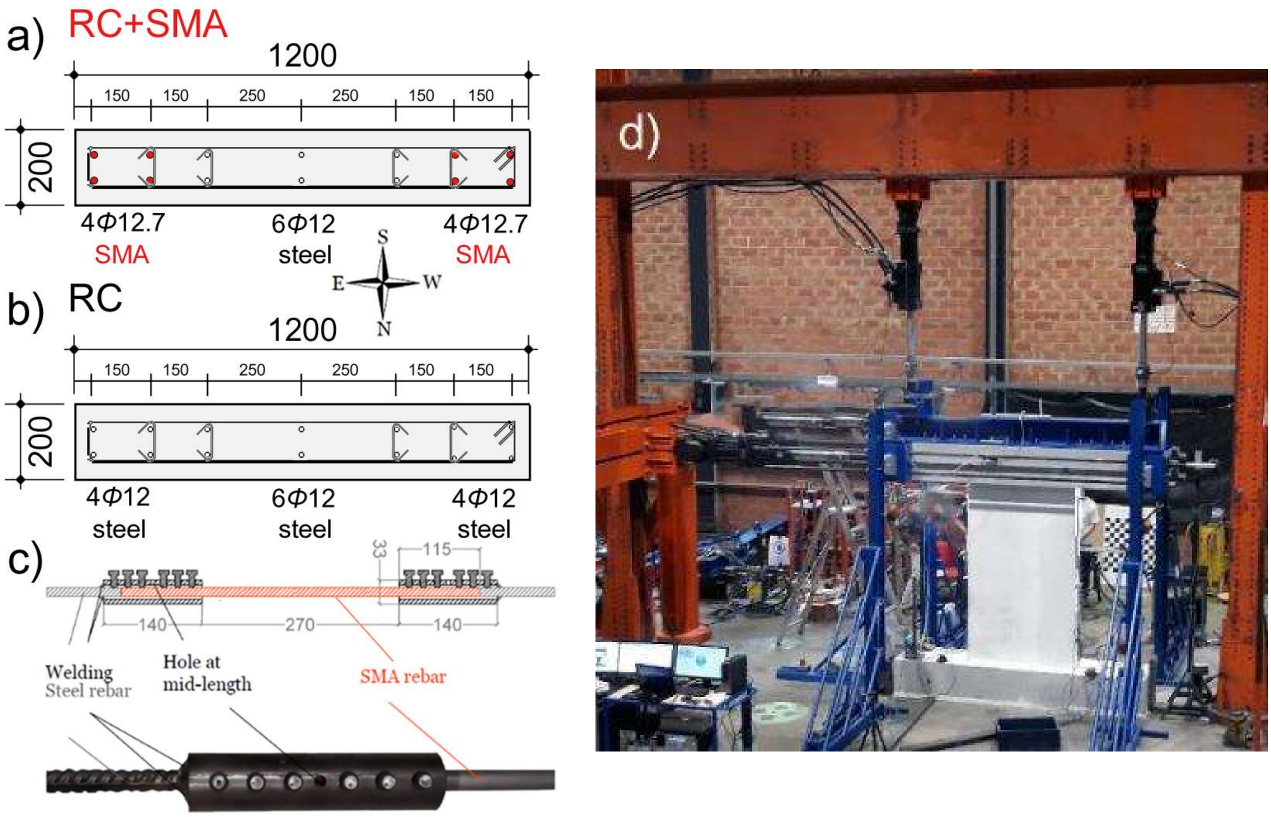

Figure 1. Cross-section and longitudinal reinforcement layout of test units (a) RC+SMA and (b) RC, (c) SMA-steel rebar assembly and mechanical coupler photo, and (d) test setup assembly at the technological platform LEMSC for the test of the two walls

A RC wall unit detailed with SMA bars in the boundary ends (denoted unit "RC+SMA") was tested by some of the authors [25]. The elevation view of the specimen in the testing position is given in Figure 1d, which had a specimen height (h_s) of 2000 mm, wall length (L_w) of 1200 mm, and thickness (t_w) of 200 mm. The concrete strength (f_c) of the RC+SMA wall specimen was reportedly 49.2 MPa. Two vertical actuators applied a total axial load (P) of 350 kN, corresponding to an axial load ratio ($ALR = P / f'_c A_g$) of approximately 3%. Importantly, the vertical actuators also applied a moment to increase the shear span (L_v) of the wall, resulting in an effective height (H_e) of approximately 4.32 m. A conventional wall, detailed with reinforcing steel (denoted wall unit "RC"), was also tested for comparative purposes, which was detailed with two layers of longitudinal reinforcement as shown in Figure 1b. The diameter of the conventional longitudinal steel bars was 12 mm, whereas the transverse reinforcement consisted of 8 mm bars spaced at 150 mm. Some confinement was also provided in the boundary end regions using 8mm diameter hooped bars spaced at 150 mm. SMA rebars with bar diameter (d_{bl}) of 12.7 mm replaced the conventional steel in the two outer-pairs of bars in the boundary end regions and over a height of 270 mm from the base (Figure 1a). Budget constraints were largely responsible for the short length of the SMA bars used, which were much smaller than the expected yielding length of the wall. Information on the experimental observations can be found in the corresponding published paper [25].

A VecTor2 FE model of the RC+SMA wall unit was employed to simulate the reverse-cyclic behaviour and overall seismic performance. An element size corresponding to $0.33t_w$ was adopted for the walls based on a mesh sensitivity analysis that was conducted [33]. As there is no option in VecTor2 to apply a moment, the modelled loading beam was extrapolated to the effective wall height. All nodes at a height of 4.32 m from the base were subjected to both axial load (held constant throughout analysis) and lateral displacement, which corresponded to the shear span used experimentally. A displacement-controlled, reverse-cyclic protocol was used numerically to achieve the same loading protocol applied experimentally. The numerical force-displacement response from VecTor2 for the RC+SMA specimen is illustrated in Figure 2a. Superimposed in this figure are the experimental results from Almeida *et al.* [25]. A reasonable estimate of the force-displacement response of this wall is obtained numerically. As can be observed, the onset of failure, caused by fracture of the outermost layer of reinforcing steel bars, occurred during the cycle towards a drift of approximately 2.4%, corresponding to a reduction in the force capacity. While there was some instability and convergence issues once the steel rebar was estimated to have fractured, the numerical simulation continued to the same drift in the opposite direction, ultimately causing global failure of the wall and causing the analysis to stop. These numerical observations are similar to the experimental results, where steel rebar fracture could be heard as the wall progressed towards a drift of 2.0% and global failure occurring soon after. The VecTor2 simulations also provide reasonable estimates of the residual displacements of the wall, as indicated in Figure 2b. While there are discrepancies between the FE model and the experimental results of the pinching response, which is due to the material model simulating the SMA rebar [33], the residual displacements of the wall are still reasonably captured. The numerical residual displacement results in Figure 2b have been calculated at two different heights: (i) the effective height of 4.32 m and (ii) the specimen height of 2.20 m. The latter height corresponds to that used experimentally in Almeida *et al.* [25] to calculate the in-plane drift and residual displacements, as only the lower section of the wall was tested (i.e., an applied moment was used to increase the shear span). The limiting drift of 0.005 rad (or 0.5%) [36] is based on an average drift, which is indicated in Figure 2b with the red-dashed lines (depending on the height). Importantly, the numerical residual displacements are estimated to be greater than this residual displacement limit for in-plane drift levels of around 2.0−2.5%, which correlates reasonably well to the experimental observations. The residual displacements of the companion wall, unit RC, tested by Almeida et al. [25] and detailed with conventional steel are also provided in Figure 2b ("RC-Steel" in the corresponding legend), which show that the permissible limit is reached at a much-reduced average in-plane drift of approximately 1.0%.

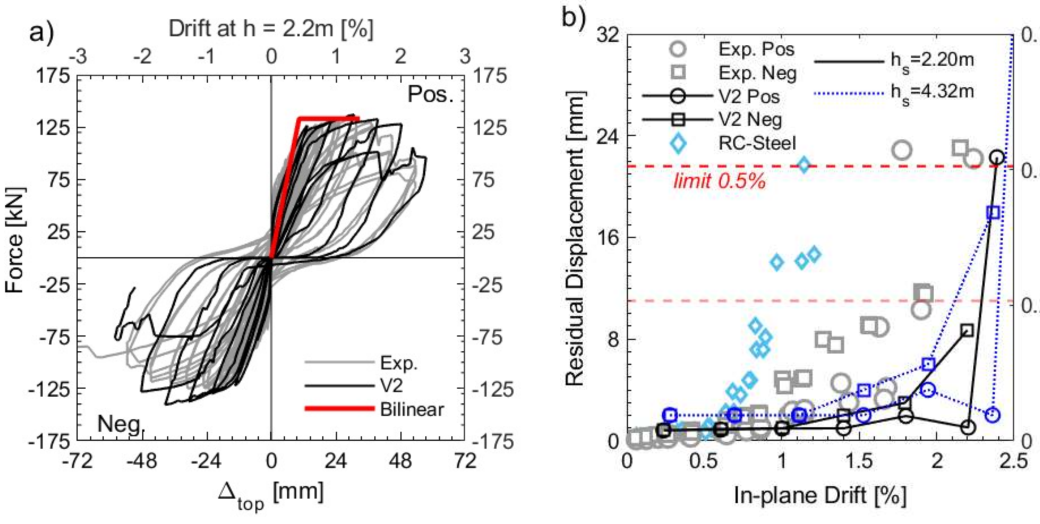

Figure 2. Experimental ("Exp.") and numerical ("V2") results for the RC+SMA wall specimen from Almeida et al. [33] (a) force-displacement hysteresis and (b) residual displacements as a function of in-plane drift, where "Pos" and "Neg" corresponds to the positive and negative directions of top wall displacement. The blue diamonds ("RC-Steel") correspond to the residual displacements of the tested companion wall with conventional steel reinforcement. The bilinear curve in red is obtained from plastic hinge analysis

FUTURE RESEARCH

F_e–based Shape Memory Alloys

The costs associated with NiTi-based SMAs appears to be one of the barriers for widespread implementation as a construction material in the building stock. While the increasing demand for NiTi-based SMAs has depreciated its price significantly [37], iron (F_e) based SMAs have the potential to significantly decrease the cost for applications in civil engineering design [38]. Only recently has a ferrous alloy been reported that can exhibit the highly desired superelastic effects at room temperature [39]. Compared to the NiTi-based SMAs, the martensite transformation mechanism of F_e-based SMAs is fundamentally different; the F_e-SMA is generally considered to be inferior to the NiTi-SMA in terms of recovery capability [40]. For example, a recovery strain of 2.5% has been reported [40] without "training" the alloy (i.e., thermomechanical cycling [41]). However, with training, strain recoveries of up to 4.5% have also been reported [42]. To put this into context, in contrast to conventional steel bars with elastic strain limits of approximately 0.25%, some F_e-based SMA bars have been shown to perform with excellent pseudoelastic behaviour with recoverable strains of over 5% [43]. In fact, a F_e-based SMA has been developed that shows a recovery strain of over 13% at room temperature and a very high tensile strength of 1200 MPa, placing this alloy at the cutting edge of knowledge as far as new materials are concerned [44, 45]. In addition, the mixing of chromium into some Fe-based alloys has been shown to effectively improve the corrosion resistance of the material [46-48].

An interdisciplinary experimental program will begin mid-2023 at UCLouvain, which will focus on the seismic performance of RC walls detailed with F_e-based SMAs. The experimental program includes (i) characterising the hysteretic behaviour of F_e-based SMA rebars, (ii) pull-out tests on several concrete cylinder specimens to determine the bond strength of the embedded F_e-based SMA bars, and more generally develop the bond-slip relation; state-of-the-practice fiber-optic sensors will be used to acquire high-resolution strain profiles of the rebar embedded in the concrete – this technology was recently used by some of the authors to derive salient strain profiles of rebars embedded in RC walls [49], (iii) RC prisms that idealise the boundary ends of walls will be tested under uniaxial loading to assess key failure modes of flexurally-dominated walls, (iv) assess the seismic performance and residual displacement capacity of two planar RC walls detailed with F_e-based rebars by conducting large-scale experimental tests on specimens subjected to quasi-static loading, (v) conduct a parametric study of RC walls detailed with F_e-based SMAs using state-of-the-art finite element modelling. This project is sponsored by a Marie Skłodowska-Curie Actions Postdoctoral Fellowship.

Shake Table Test on RC+SMA Wall

The authors, as part of a larger user group, will conduct experimental dynamic tests on two large-scale RC U-shaped core walls in the latter part of 2023 using a shake table at the National Laboratory for Civil Engineering (LNEC), Portugal. This experimental program will be funded mainly by the Engineering Research Infrastructures for European Synergies (ERIES) Transnational Access program. Furthermore, these dynamic tests will be a continuation of an experimental program conducted at UCLouvain, Belgium, which involved quasi-static tests on two RC U-shaped core walls subjected to axial-flexural and axial-torsional loading [49-51]. The proposed dynamic tests units are illustrated in Figure 3, which have the same geometry and approximately the same reinforcement detailing as the quasi-static tests. To comply with the 40-ton maximum payload of the table, 28 tons of additional mass will be placed at the top of the wall. This experimental program provides an exciting opportunity to replace the steel rebars of one of the test units with SMA rebars. As shown in Figure 3b, the longitudinal rebars at the base and in boundary regions of the non-planar unit will be replaced with Ni-Ti SMAs. Several restrictions (e.g., budget, displacement-capacity, coupling-technique) exist such that the SMA rebars will extend over a limited height from the foundation up the wall – this length has yet to be determined.

Given the paucity of experimental research that has dynamically tested RC structures detailed with SMAs (e.g., [52]), it is hoped that, of the many outputs of this research program, the test results will justify the need for explicit consideration of residual displacements, and their minimisation, in future building codes. Importantly, an international blind prediction competition will be launched focusing on these dynamic tests, where the modelling approaches submitted by the participants will be collected and analysed for a critical discussion of the state-of-the-art practice. A special issue has also been launched in early-2023 in the *Bulletin of Earthquake Engineering* that focuses on the advances on modelling and design of RC structural wall systems and the blind- and post-diction simulations of U-shaped wall tests.

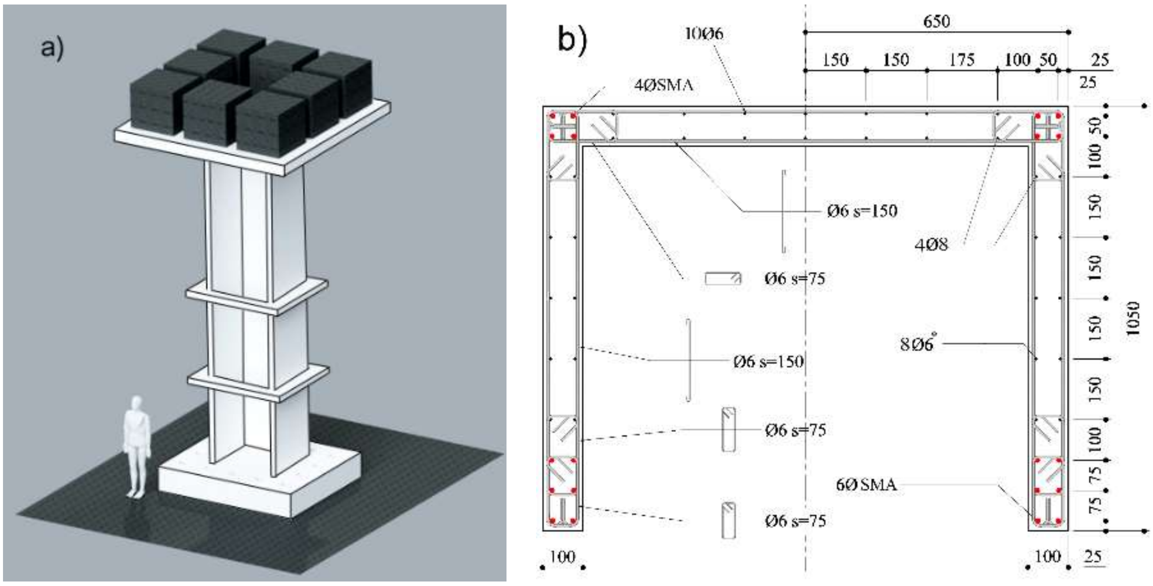

Figure 3. Preliminary proposal of the RC+SMA U-shaped wall unit to be tested as part of the ALL4wALL project, funded by ERIES (a) elevation 3-dimensional view (b) geometry and reinforcement detailing of the 1:2 scaled unit

Concrete structures with fibre-reinforced polymer reinforcement: Hybrid FRP-SMA composite

Since the late 1980s, fibre-reinforced polymers (FRP) rebars have emerged as a non-corrodible alternative to conventional steel rebars. With recent developments in polymers and manufacturing process, this alternative reinforcement has been gaining traction, and a drastic increase of its use in Europe is expected to be seen. In fact, the next generation of Eurocodes will include, for the first time, the design of RC members with FRP reinforcement. One of the critical challenges for the FRP-RC structures is their seismic behaviour. The brittle, linear-elastic response of the FRP reinforcement to rupture, raises concerns regarding their use in seismic regions. Significant amount of research is hence expected in the next decades to increase the ductility capacity of these structures. It can be achieved from capacity-design considerations coupled with well-confined concrete and/or from key local replacement of FRP reinforcement by improved-FRP or SMA rebars. This section describes some of the work that is being carried out regarding the former, whereas the following section addresses some of the planned experimental tests on FRP-RC walls partially reinforced with SMA rebars.

In order to try to convey some ductility, recentering, and energy-dissipation capacity to FRP rebars, an ongoing study focuses on the fabrication and characterization of four different configurations of SMA hybrid composite samples. A hybrid Twill 2/2 carbon-kevlar/epoxy prepreg (KC213 Sergé Carb/Aramide 213gr/m² 120cm, Sicomin, France) is used as the base material for the FRP. Superelastic shape memory alloy wires (TiNiCo, SAES Getters, US) with 125 µm of diameter were imbedded in between prepreg layers. The SMA were pre-strained via a specifically designed clamping device. The SMA wires were used with different volume ratios, stacked and stitched configurations. The FRP-SMA hybrid composite was then manufactured using cure cycle (heated to 100°C with 2°C/min heating rate, under 1 bar; then from 100°C to 125°C under 2 bars, with 1h dwell and cold down with 2°C/min) by contact moulding at hot press. The hybrid FRP functionalized by SMA composite has been cut to the different kind of samples and characterized in static (tensile and bending) and dynamic (vibration) tests. Static tensile and bending tests are conducted using a 100 kN hydraulic Zwick bench with a displacement control speed of 2 mm/min, according to ISO 527-4 and ISO 14125 standards, respectively. The mechanical characteristics, residual deflection, energy dissipation until failure, ductility capacity, among others, are then compared. It was concluded that even a small quantity of SMA wires (2%) has a considerable impact, and that in particular the disposition of the wires in the sample configuration plays a crucial role. The increasing amount of SMA seems to improve the deflection recovery.

Concerning the dynamic tests, a series of experimental vibration tests have been conducted at the Quartz Laboratory of ISAE-Supméca (France) using the electromagnetic shaker Tira TV59320 and an impacting hammer. The FRP and the different FRP-SMA composite specimens were cut by a water-jet machine into rectangular beams of size 230 x 15 x 2 mm^3. The beams were then clamped at one edge and kept free on the other one along the major dimension. The clamped edge was fixed on the shaking table perpendicularly to the motion direction. One accelerometer was fixed at the top of the free edge and one on the clamping. The goals of the tests were to perform an experimental modal analysis and to verify the linearity of vibration around the first modal frequency. To this end, the beam dynamics were tested under different loading cases and amplitudes, notably in case of shock, initial displacement of the free edge, random excitation and frequency sweep. For all cases, the first modal frequencies and modal damping were estimated by using the Frequency Domain Decomposition [53]. Some of the preliminary results are as follows: the FRP-SMA composites exhibit a lower first modal frequency comparable to the FRP; the modal frequency is little affected by the external amplitude; on the other hand, as expected, the damping ratio of the FRP-SMA composite is highly amplitude dependent. Regarding this latter point, further research is needed to understand the effect of the SMA properties on the hybrid composite dynamics, in particular with respect to its damping capability. Moreover, the utilization of more sensors, physical or virtual in the case of video analysis, are necessary for the identification of possible nonlinear normal modes [54].

A dedicated manuscript will be soon submitted for publication in a specialised journal with a full description of this new material, and the results obtained.

Concrete structures with fibre-reinforced polymer reinforcement: Experimental tests of walls detailed with GFRP and SMA reinforcement

Regarding the combination of SMA rebars with FRP rebars in FRP-RC walls, and as far as the authors are aware, it has not yet been explored. However, several reasons point to a potentially successful partnership worth exploring: (i) as discussed, SMA rebars can be placed in the wall base boundary element regions over a restricted plastic hinge length, resulting in an extremely reduced required quantity of SMA rebars at the building scale; (ii) capacity-design principles can be readily employed to guarantee that FRP reinforcement above the SMA plastic hinge region remains elastic; (iii) similar Young's modulus between SMA and FRP rebars, as well as corrosion-resistance. In view of the above, large-scale experimental wall tests are planned at UCLouvain for the end of 2023 / beginning of 2024, where the mentioned association between SMA and glass fibre reinforced polymer (GFRP) rebars will be explored. Two H-shaped units are foreseen: one fully reinforced with GFRP rebars, another with SMA reinforcement locally replacing GFRP rebars in key regions at the base. The walls will be subjected to a vertical axial load and a quasi-static reverse-cyclic displacement-controlled lateral loading protocol. The SMA+GFRP rebars will be instrumented with distributed optical fibre sensors.

CONCLUSIONS

Future design and construction of reinforced concrete structures will need to consider longer service lives, which requires, among many things, some durability considerations and more refined seismic performance criteria. Minimising residual displacements is key to post-earthquake repairability and serviceability of structures and will be an important performance criterion for building codes in the future.

This paper has summarised some areas of research amongst the authors investigating smart materials, namely shape memory alloys (SMAs) and fibre reinforced polymers (FRPs), as a potential replacement of reinforcing steel in concrete structures. These materials have the potential to improve the corrosion resistance of the structure and, in the event of large earthquake ground motions, reduce the residual displacements of a building. Some of the present and ongoing research projects summarised in this paper include: (i) a novel connection method between steel and SMA bars, using inertia friction welding, which provides promising results to avoid the use of mechanical couplers, (ii) recent advanced numerical modelling of walls with SMA rebars with a focus on the simulation of residual displacements, (iii) some comments on the foreseen application of cost-effective iron-based superelastic SMA rebars, which will be explored in an upcoming project, (iv) an overview of an upcoming shake-table test of a 40-ton large-scale RC U-shaped core wall detailed with SMA rebars, (v) the development of a novel hybrid composite FRP-SMA – alleviating some of the material disadvantages of the existing FRP rebar materials, and (vi) an upcoming test program of walls detailed with GFRP and SMA reinforcement.

While preliminary results are promising, further experimental research on RC structures using these smart materials is required to confirm the performance. As more experimental data becomes available, more numerical studies can be conducted to further refine some of the findings and recommendations made from these different research investigations.

REFERENCES

[1] Awoyera P, Adesina A, Olalusi OB, Viloria A. Reinforced concrete deterioration caused by contaminated construction water: An overview. Engineering Failure Analysis. 2020:104715.
[2] Mehta PK, Monteiro PJ. Concrete: microstructure, properties, and materials: McGraw-Hill Education; 2014.
[3] Hanif MU, Ibrahim Z, Ghaedi K, Hashim H, Javanmardi A. Damage assessment of reinforced concrete structures using a model-based nonlinear approach – A comprehensive review. Construction and Building Materials. 2018;192:846-65. doi:10.1016/j.conbuildmat.2018.10.115
[4] UN. World Population Prospects: The 2019 Revision. Volume 1. United Nations, Department of Economics and Social Affairs, Population Division. 2019.
[5] Dean B, Dulac J, Petrichenko K, Graham P. Global status report 2016: towards zero-emission efficient and resilient buildings. 2017.
[6] Statista. Available online: https://www.statista.com/statistics/219343/cement-production-worldwide/ (Accessed on 03 November 2021). 2019.
[7] Yang Y, Li Z, Zhang T, Wei J, Yu Q. Bond-slip behavior of basalt fiber reinforced polymer bar in concrete subjected to simulated marine environment: effects of BFRP bar size, corrosion age, and concrete strength. International Journal of Polymer Science. 2017;2017.

[8] Praneeth S, Saavedra L, Zeng M, Dubey BK, Sarmah AK. Biochar admixtured lightweight, porous and tougher cement mortars: Mechanical, durability and micro computed tomography analysis. Science of The Total Environment. 2021;750:142327. doi:10.1016/j.scitotenv.2020.142327
[9] IPCC. Climate change 2014: Synthesis report. Contribution of working groups I, II and III to the fifth assessment report of the intergovernmental panel on climate change. Intergovernmental Panel on Climate Change, Geneva, Switzerland. 2014.
[10] Asadi E, Shen Z, Zhou H, Salman A, Li Y. Risk-informed multi-criteria decision framework for resilience, sustainability and energy analysis of reinforced concrete buildings. Journal of Building Performance Simulation. 2020;13(6):804-23.
[11] Biondini F, Camnasio E, Titi A. Seismic resilience of concrete structures under corrosion. 2015;44(14):2445-66. doi:10.1002/eqe.2591
[12] Nataraj S, Hogan L, Scott A, Ingham J. Simplified Mechanics-Based Approach for the Seismic Assessment of Corroded Reinforced Concrete Structures. Journal of Structural Engineering. 2022;148(3):04021296.
[13] D'Alessandro A, Luzio D, D'Anna G. Urban MEMS based seismic network for post-earthquakes rapid disaster assessment. Advances in Geosciences. 2014. doi:10.5194/adgeo-40-1-2014
[14] Ritchie H, Roser M. Natural Disasters. Our World in Data. 2014.
[15] Muir-Wood R. The Christchurch earthquakes of 2010 and 2011. The Geneva risk reports. Risk and insurance research. Extreme events and insurance: 2011 Annus horribilis. Courbage C, Stahel WR, Geneva. 2015.
[16] Gonzalez R, Stephens M, Toma C, Elwood K, Dowdell D. Post-earthquake Demolition in Christchurch, New Zealand: A Case-Study Towards Incorporating Environmental Impacts in Demolition Decisions. Advances in Assessment and Modeling of Earthquake Loss2021. p. 47-64.
[17] Kawashima K. Seismic design and retrofit of bridges. Bulletin of the New Zealand Society for Earthquake Engineering. 2000;33(3):265-85.
[18] Fujino Y, Hashimoto S, Abe M. Damage analysis of Hanshin Expressway viaducts during 1995 Kobe earthquake. I: Residual inclination of reinforced concrete piers. Journal of Bridge Engineering. 2005;10(1):45-53.
[19] Rosenblueth E, Meli R. The 1985 mexico earthquake. Concrete international. 1986;8(5):23-34.
[20] Mitchell D, DeVall RH, Saatcioglu M, Simpson R, Tinawi R, Tremblay R. Damage to concrete structures due to the 1994 Northridge earthquake. Canadian journal of civil engineering. 1995;22(2):361-77.
[21] Di Ludovico M, De Martino G, Prota A, Manfredi G, Dolce M. Damage Assessment in Italy, and Experiences After Recent Earthquakes on Reparability and Repair Costs. Advances in Assessment and Modeling of Earthquake Loss: Springer, Cham; 2021. p. 65-84.
[22] de la Llera JC, Rivera F, Mitrani-Reiser J, Jünemann R, Fortuño C, Ríos M, et al. Data collection after the 2010 Maule earthquake in Chile. B Earthq Eng. 2017;15(2):555-88.
[23] Angst UM, Hooton RD, Marchand J, Page CL, Flatt RJ, Elsener B, et al. Present and future durability challenges for reinforced concrete structures. Materials and Corrosion. 2012;63(12):1047-51. doi:10.1002/maco.201206898
[24] International Energy Agency. Iron and Steel Technology roadmap: Towards more sustainable steelmaking. Technology report ieaorg. 2020.
[25] Almeida JPd, Steinmetz M, Rigot F, de Cock S. Shape-memory NiTi alloy rebars in flexural-controlled large-scale reinforced concrete walls: Experimental investigation on self-centring and damage limitation. Engineering Structures. 2020;220:110865. doi:10.1016/j.engstruct.2020.110865
[26] Abdulridha A, Palermo D. Behaviour and modelling of hybrid SMA-steel reinforced concrete slender shear wall. Engineering Structures. 2017;147:77-89. doi:10.1016/j.engstruct.2017.04.058
[27] Cortés-Puentes L, Zaidi M, Palermo D, Dragomirescu E. Cyclic loading testing of repaired SMA and steel reinforced concrete shear walls. Engineering Structures. 2018;168. doi:10.1016/j.engstruct.2018.04.044
[28] Kian MJT, Cruz-Noguez C. Reinforced Concrete Shear Walls Detailed with Innovative Materials: Seismic Performance. Journal of Composites for Construction. 2018;22(6):04018052. doi:10.1061/(ASCE)CC.1943-5614.0000893
[29] Raza S, Shafei B, Saiid Saiidi M, Motavalli M, Shahverdi M. Shape memory alloy reinforcement for strengthening and self-centering of concrete structures—State of the art. Construction and Building Materials. 2022;324. doi:10.1016/j.conbuildmat.2022.126628
[30] Dahal PK, Tazarv M. Mechanical bar splices for incorporation in plastic hinge regions of RC members. Construction and Building Materials. 2020;258. doi:10.1016/j.conbuildmat.2020.120308
[31] Tazarv M, Saiidi MS. Seismic design of bridge columns incorporating mechanical bar splices in plastic hinge regions. Engineering Structures. 2016;124. doi:10.1016/j.engstruct.2016.06.041
[32] Lezaack MB, Simar A, Marchal Y, Steinmetz M, Faes K, Pacheco de Almeida J. Dissimilar friction welding of NiTi shape memory alloy and steel reinforcing bars for seismic performance. Science and Technology of Welding and Joining. 2022;27(6). doi:10.1080/13621718.2022.2061692
[33] Hoult RD, Almeida JPd. Residual displacements of reinforced concrete walls detailed with conventional steel and shape memory alloy rebars. Engineering Structures. 2022;256. doi:10.1016/j.engstruct.2022.114002
[34] Wong P, Vecchio F, Trommels H. Vector2 and FormWorks User Manual. Department of Civil Engineering, University of Toronto. 2013.
[35] Vecchio F. Disturbed Stress Field Model for Reinforced Concrete: Formulation. Journal of Structural Engineering. 2000;126(9):1070-7.

[36] McCormick J, Aburano H, Ikenaga M, Nakashima M, editors. Permissible residual deformation levels for building structures considering both safety and human elements. Proceedings of the 14th world conference on earthquake engineering; 2008; Beijing, China: WCEE.

[37] Ozbulut OE, Hurlebaus S, DesRoches R. Seismic response control using shape memory alloys: a review. Journal of Intelligent Material Systems and Structures. 2011;22(14):1531-49.

[38] Cladera A, Weber B, Leinenbach C, Czaderski C, Shahverdi M, Motavalli M. Iron-based shape memory alloys for civil engineering structures: An overview. Construction and Building Materials. 2014;63:281-93. doi:10.1016/j.conbuildmat.2014.04.032

[39] Tanaka Y, Himuro Y, Kainuma R, Sutou Y, Omori T, Ishida K. Ferrous polycrystalline shape-memory alloy showing huge superelasticity. Science. 2010;327(5972):1488-90.

[40] Wang B, Zhu S. Cyclic behavior of iron-based shape memory alloy bars for high-performance seismic devices. Engineering Structures. 2021:113588.

[41] Van Caenegem N, Verbeken K, Segers D, Houbaert Y. Improvement of the Shape Memory Effect in Fe-based Alloys by Training. steel research international. 2008;79(4):314-20.

[42] Maruyama T, Kubo H. Ferrous (Fe-based) shape memory alloys (SMAs): properties, processing and applications. Shape Memory and Superelastic Alloys: Elsevier; 2011. p. 141-59.

[43] Omori T, Ando K, Okano M, Xu X, Tanaka Y, Ohnuma I, et al. Superelastic effect in polycrystalline ferrous alloys. Science. 2011;333(6038):68-71.

[44] Ma J, Karaman I. Expanding the repertoire of shape memory alloys. Science. 2010;327(5972):1468-9.

[45] Ma J, Hornbuckle B, Karaman I, Thompson G, Luo Z, Chumlyakov YI. The effect of nanoprecipitates on the superelastic properties of FeNiCoAlTa shape memory alloy single crystals. Acta materialia. 2013;61(9):3445-55.

[46] Otsuka H, Yamada H, Maruyama T, Tanahashi H, Matsuda S, Murakami M. Effects of alloying additions on Fe-Mn-Si shape memory alloys. ISIJ international. 1990;30(8):674-9.

[47] Li H, Dunne D. New corrosion resistant iron-based shape memory alloys. ISIJ international. 1997;37(6):605-9.

[48] Lin H, Lin K, Lin C, Ouyang T. The corrosion behavior of Fe-based shape memory alloys. Corrosion science. 2002;44(9):2013-26.

[49] Hoult R, Bertholet A, Almeida JPd. Core versus Surface Sensors for Reinforced Concrete Structures: A Comparison of Fiber-Optic Strain Sensing to Conventional Instrumentation. Sensors. 2023;23(3). doi:10.3390/s23031745

[50] Hoult R, Doneux C, Almeida JPd. Tests on Reinforced Concrete U-shaped Walls Subjected to Torsion and Flexure. Submitted to Earthquake Spectra. 2023.

[51] Hoult R, Correia AA, Almeida JPd. Beam-Truss Models to Simulate the Axial-Flexural-Torsional Performance of RC U-Shaped Wall Buildings. CivilEng. 2023;4(1). doi:10.3390/civileng4010017

[52] Noguez CAC, Saiidi MS. Shake-Table Studies of a Four-Span Bridge Model with Advanced Materials. Journal of Structural Engineering. 2012;138(2):183-92. doi:10.1061/(ASCE)ST.1943-541X.0000457

[53] Rune B, Lingmi Z, Palle A. Modal identification of output-only systems using frequency domain decomposition. Smart Materials and Structures. 2001;10(3):441. doi:10.1088/0964-1726/10/3/303

[54] Kerschen G, Peeters M, Golinval JC, Vakakis AF. Nonlinear normal modes, Part I: A useful framework for the structural dynamicist. Mechanical Systems and Signal Processing. 2009;23(1):170-94. doi:10.1016/j.ymssp.2008.04.002